Plasma-induced asymmetric self-phase modulation and modulational instability in gas-filled hollow-core photonic crystal fibers

Saleh, Mohammed Fathy; Chang, Wonkeun; Travers, John C.; Russell, Philip St. J.; Biancalana, Fabio

Published in:
Physical Review Letters

DOI:
10.1103/PhysRevLett.109.113902

Publication date:
2012

Plasma-Induced Asymmetric Self-Phase Modulation and Modulational Instability in Gas-Filled Hollow-Core Photonic Crystal Fibers

Mohammed F. Saleh,[1] Wonkeun Chang,[1] John C. Travers,[1] Philip St. J. Russell,[1,2] and Fabio Biancalana[1]

[1]*Max Planck Institute for the Science of Light, Günther-Scharowsky str. 1, 91058 Erlangen, Germany*

[2]*Department of Physics, University of Erlangen-Nuremberg, Erlangen, Germany*

(Received 9 April 2012; published 13 September 2012)

We study theoretically the propagation of relatively long pulses with ionizing intensities in a hollow-core photonic crystal fiber filled with a Raman-inactive noble gas. Because of photoionization, an extremely asymmetric self-phase modulation and a new kind of "universal" plasma-induced modulational instability appear in both normal and anomalous dispersion regions. We also show that it is possible to spontaneously generate a plasma-induced continuum of blueshifting solitons, opening up new possibilities for pushing supercontinuum generation towards shorter and shorter wavelengths.

DOI: 10.1103/PhysRevLett.109.113902 PACS numbers: 42.65.Tg, 42.81.Dp, 52.35.Sb

Introduction —Hollow-core photonic crystal fibers (HC-PCFs) have extended the fields of linear and nonlinear fiber optics well beyond the interaction of light with solid media [1]. The feasibility of designing and fabricating various HC-PCF structures allows distinct special nonlinear and dispersive properties of these fibers [2]. For instance, kagome HC-PCFs typically show high confinement of light in the core with relatively low loss and low group velocity dispersion (GVD) in the visible and near-IR [2–4]. Recently, these fibers, filled with noble (Raman-free) gases, have been used in a series of groundbreaking experiments. Few-μJ femtosecond-scale pulses were launched into argon-filled cm-long HC-PCFs, leading to the observation of a unique photoionization-induced soliton self-frequency blueshift [5]. These experiments are accurately described by a unidirectional pulse propagation equation (UPPE) based on the full electric field [6,7], which is complemented by sophisticated tunneling and multiphoton ionization models [8]. The UPPE model can, however, be reduced to a simple pair of coupled equations for the envelope of the electric field and the ionization fraction [9,10], and remarkable qualitative agreement with the full model and with experiments was obtained.

The well-known Raman self-frequency redshift in solid-core fibers acts on a soliton by continuously shifting its central frequency toward longer wavelengths via inelastic scattering with optical phonons provided by the medium, leading to a decrease of the soliton energy, while the photon number remains constant [11–13]. In contrast, the photoionization-induced self-frequency blueshift acts on a soliton by continuously increasing its central frequency via energy received from the created plasma. In order for this action to take place spontaneously, without violating the second law of thermodynamics, a reduction in the photon number, or in other words an ionization-induced loss, must take place [5,9,10].

In this Letter, we show theoretically that when the gas is excited by relatively *long* pulses at ionizing intensities, new kinds of self-phase modulation (SPM) and modulational instability (MI) emerge during propagation. Moreover, once the initial stage of instability is over, a "shower" of hundreds of solitons, each undergoing an ionization-induced self-frequency blueshift, pushes the supercontinuum spectrum towards shorter and shorter wavelengths. Such a *blueshifting* plasma-induced continuum has some similarities with the *redshifting* Raman-induced continuum driven by the Raman self-frequency shift in conventional solid-core fibers [14–16], although the underlying physical processes are dramatically different.

Governing equations.—The propagation of light in a HC-PCF filled with an ionizable Raman-inactive gas can be modeled by the following pair of normalized coupled equations [9,10]:

$$i\partial_\xi \psi + \hat{D}(i\partial_\tau)\psi + |\psi|^2\psi - \phi\psi + i\alpha\psi = 0, \quad (1)$$

$$\partial_\tau \phi = \sigma(\phi_T - \phi)\Delta|\psi|^2\Theta(\Delta|\psi|^2) - r\phi^2, \quad (2)$$

where ψ is the electric field envelope, ϕ is a quantity proportional to the number of electrons created by the photoionization process, ξ is the normalized longitudinal coordinate along the fiber, τ is time in a reference frame moving with the input pulse group velocity, $\hat{D}(i\partial_\tau)$ is the full GVD operator, $\alpha = \kappa(\phi_T - \phi)[1 - |\psi|^2_{\rm th}/|\psi|^2]\Theta(\Delta|\psi|^2)$ is the ionization-induced loss, κ is a normalization factor (see also Refs. [9,10,17] for extensive details), Θ is the Heaviside step function, $\Delta|\psi|^2 \equiv |\psi|^2 - |\psi|^2_{\rm th}$, $|\psi|^2_{\rm th}$ is the normalized ionization threshold intensity, σ and ϕ_T are constants that can be determined through the tunneling ionization equation rate [9,10], and r is a coefficient regulating the recombination between free electrons and ions, which is a two-particle process and hence depends on ϕ^2.

Equations (1) and (2) yield excellent qualitative agreement with experiments using ultrashort input pulses [5],

accurately predicting the dynamics of soliton formation and the plasma-induced soliton self-frequency blueshift [9,10]. At the core of the model is the assumption that the dynamics are dominated by tunneling photoionization, and that the ionization rate can be described by a linear function corrected by a Heaviside function that takes into account the threshold intensity [3,9,10]. Although the relatively long pulses considered here are expected to drive some multiphoton ionization, comparisons of Eqs. (1) and (2) to UPPE simulations using the more general Yudin-Ivanov ionization model [8]—which we present at the end of this Letter—show excellent agreement.

Plasma-induced asymmetric self-phase modulation—Ionization-induced SPM can be studied by simplifying Eqs. (1) and (2) for the case of weak dispersion and long input pulse durations t_0. In this situation (natural for kagome-PCFs since the GVD is very small), the nonlinearity initially dominates over the GVD, since the "soliton number" N (i.e., the input pulse energy) is large [17], and the second term in Eq. (1) can be safely neglected in the very initial stage of propagation. In kagome-PCFs, input energies such that $N > 100$ are realistically achievable for pulses with >0.5 ps duration. Neglecting also the recombination process, Eq. (2) can be written as $\phi(\tau) = \phi_T\{1 - \exp[-\sigma \int_{-\infty}^{\tau} \Delta|\psi(\tau')|^2\Theta(\Delta|\psi(\tau')|^2)d\tau']\}$. For small values of σ, Eqs. (1) and (2) can be reduced to a single integro-differential equation,

$$i\partial_\xi\psi + |\psi|^2\psi - \eta\psi\int_{-\infty}^{\tau}\Delta|\psi(\tau')|^2\Theta(\Delta|\psi(\tau')|^2)d\tau' + i\alpha\psi = 0, \quad (3)$$

where $\eta = \sigma\phi_T$. By temporarily ignoring the losses (which do not change the qualitative picture that we are going to describe, but only saturate the SPM spectrum after a certain distance), Eq. (3) can be solved by substituting $\psi(\xi,\tau) = V(\xi,\tau)\exp[i\varphi_{\rm NL}(\xi,\tau)]$ [17], where V and $\varphi_{\rm NL}$ are the amplitude and the nonlinear phase of the pulse. Separating the real and the imaginary parts, and performing the integrations results in $V(\xi,\tau) = \psi(0,\tau)$, $\varphi_{\rm NL}(\xi,\tau) = \xi[|V|^2 - \int_{-\infty}^{\tau}\Delta|V(\tau')|^2\Theta(\Delta|V(\tau')|^2)d\tau']$ and $\Delta|V|^2 = |V|^2 - |\psi|^2_{\rm th}$. We will show below that such a nonlinear phase can induce strong spectrally asymmetric SPM at a rate that is large compared to the background Kerr nonlinearity. To this end we compute the mean frequency $\langle\Omega\rangle$, and the variance $(\Delta\Omega)^2 = \langle\Omega^2\rangle - \langle\Omega\rangle^2$ [17,18], where $\langle\Omega^k\rangle = \int\Omega^k|\Psi|^2d\Omega/\int|\Psi|^2d\Omega$, $\Psi = \mathcal{F}[\psi]$, and the symbol $\mathcal{F}$ represents the Fourier transform.

In the case of an input Gaussian pulse, $\psi(0,\tau) = \exp(-\tau^2/2\tau_0^2)$, the above parameters can be determined in closed forms. We find

$$\langle\Omega\rangle = \tfrac{1}{2}\eta\xi[\sqrt{2}\,\mathrm{erf}(\sqrt{2}\mathcal{T}) - 2|\psi|^2_{\rm th}\,\mathrm{erf}(\mathcal{T})], \quad (4)$$

$$(\Delta\Omega)^2 = \frac{1}{18\tau_0^2}(9 + 4\sqrt{3}\xi^2 - 3\xi^2\eta^2\tau_0^2\{[3\,\mathrm{erf}^2(\sqrt{2}\mathcal{T}) - 2\sqrt{3}\,\mathrm{erf}(\sqrt{3}\mathcal{T})] + 6|\psi|^2_{\rm th}[\mathrm{erf}(\mathcal{T}) - 1] \times [|\psi|^2_{\rm th}\,\mathrm{erf}(\mathcal{T}) - \sqrt{2}\mathrm{erf}(\sqrt{2}\mathcal{T})]\}), \quad (5)$$

where erf is the error function, $\mathcal{T} = T/\tau_0$, and $-T \le \tau \le T$ is the regime within which the pulse intensity exceeds the threshold intensity.

Panels (a) and (b) in Fig. 1 depict the spatial dependence of the mean frequency and the standard deviation, respectively, for different values of η, i.e., for different free-electron densities generated in the fiber. For experimentally feasible situations, η ranges approximately between 1 and 10 for noble gases. In Fig. 1(a), for $\eta = 0$, which corresponds to the absence of ionization, the mean frequency is always zero during propagation due to the well-known symmetric spectral broadening characteristic of conventional SPM [17]. As η increases (i.e., when the plasma starts to build up inside the fiber), the mean frequency moves linearly towards the blueside of the spectrum due to the ionization-induced phase modulation. This induces a strong and extremely spectrally *asymmetric* SPM, imbalanced toward the blue part of the spectrum, which is unique to the kind of gas-filled PCF waveguides studied in this Letter. This effect should be distinguished from the slight spectral asymmetry induced in the SPM by perturbations such as self-steepening, stimulated Raman scattering, and odd-order dispersion, which typically produce small blueshifted pedestals, whereas almost all the input energy goes into the red part of the spectrum [17,19]. Looking at Fig. 1(b), we find that the ionization-induced SPM broadens the spectrum significantly faster than the Kerr-based SPM. The spectral broadening process is

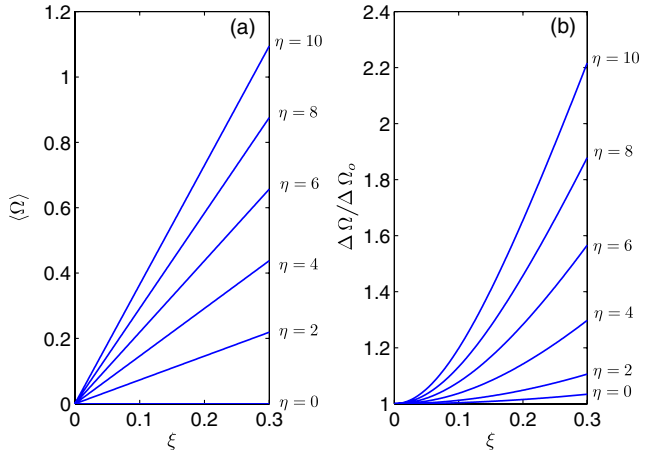

FIG. 1 (color online). Spatial dependence of (a) the mean frequency $\langle\Omega\rangle$ and (b) the frequency standard deviation $\Delta\Omega$ of a Gaussian pulse $\exp(-\tau^2/2\tau_0^2)$ with $\tau_0 = 2$. The temporal position T at which the pulse intensity can initiate photoionization is assumed to be equal to τ_0. $\Delta\Omega_0$ is the spectral width at $\xi = 0$.

limited by unavoidable ionization and fiber losses, just as in Kerr-related SPM.

Plasma-induced modulational instability—After the very initial SPM stage (described above) is over, the interplay between nonlinear and dispersive effects can lead to an instability that modulates the temporal profile of the pulse, creating new spectral sidebands referred to as MI in Refs. [20–22]. For instance, during the propagation of a continuous wave (cw) signal in an anomalously dispersive Kerr medium, perturbations to the amplitude of the carrier wave can trigger the generation of spectral sidebands, leading to the eventual breakup of the cw signal into a train of pulses [17,20,21]. MI due to the photoionization nonlinearity described by Eqs. (1) and (2) can be investigated using the standard approach presented in Refs. [17,20]. The steady state solutions of Eqs. (1) and (2), which are time independent, are found by inserting $\psi = \psi_0 e^{ik_0\xi}$ and $\phi = \phi_0$, where ψ_0 is the amplitude of a cw, with a propagation constant k_0, and ϕ_0 corresponds to the amount of plasma generated by this wave. These constants can be determined by setting the time derivatives to zero. Perturbing these steady state solutions and substituting back into Eqs. (1) and (2), one obtains the linearized equations

$$i\partial_\xi a + \frac{s}{2}\partial_\tau^2 a + \psi_0^2(a + a^*) - u\psi_0 = 0, \tag{6}$$

$$\partial_\tau u = -Fu + g(a + a^*), \tag{7}$$

where a and u are perturbations added to the amplitudes ψ_0 and ϕ_0, s is the sign of the second-order dispersion ($+1 \equiv$ anomalous dispersion, $-1 \equiv$ normal dispersion), higher-order dispersion coefficients are neglected, $F = \sigma(\psi_0^2 - |\psi|_{\text{th}}^2)\Theta(\psi_0^2 - |\psi|_{\text{th}}^2) + 2r\phi_0$, and $g = \sigma(\phi_T - \phi)\psi_0$. Substituting $a = a_1 e^{i\vartheta} + a_2 e^{-i\vartheta^*}$, $u = u_0 e^{i\vartheta} + u_0^* e^{-i\vartheta^*}$, and $\vartheta = \kappa\xi - \Omega\tau$, a set of three equations for a_1, a_2^*, and u_0 can be found. Expressing u_0 in terms of a_1 and a_2^*, we find

$$\begin{bmatrix} m_{11} & m_{12} \\ m_{21} & m_{22} \end{bmatrix}\begin{bmatrix} a_1 \\ a_2^* \end{bmatrix} = 0, \tag{8}$$

where $m_{11} = -\kappa - s\Omega^2/2 + \psi_0^2 + g\psi_0/(-F + i\Omega)$, $m_{12} = \psi_0^2 + g\psi_0/(-F + i\Omega)$, $m_{21} = -m_{12}$, and $m_{22} = -m_{11} - 2\kappa$. These equations have nontrivial solutions when

$$\kappa = \pm\frac{|\Omega|}{2}\left[\Omega^2 - 4s\left(\psi_0^2 - \frac{g\psi_0(F + i\Omega)}{F^2 + \Omega^2}\right)\right]^{1/2}, \tag{9}$$

which are the complex eigenvalues of the problem. Note that in this analysis ϕ is kept to be a real-valued positive quantity since it represents the number of electrons generated via photoionization.

Perturbations can only be amplified during propagation for frequencies which have nonreal values of propagation constant κ. In the absence of higher-order dispersion, Kerr-induced MI (e.g., in solid-core optical fibers or in HC-PCFs when excited with intensities below the ionization threshold for the gas) occurs only in the anomalous dispersion regime [17]. However, photoionization induces an unusual "universal" MI that can exist in both normal and anomalous dispersion regimes, and for any frequency, even when there is no higher-order dispersion. This universal MI arises because the ionization contribution to the destabilization of the background wave $g\psi_0/(-F + i\Omega)$ is always complex and frequency dependent, in contrast to when only the Kerr effect is present ($g = 0$). The spectral dependence of the gain, which is defined as $2\text{Im}\{\kappa\}$ for different peak powers, is shown in Fig. 2 for (a) anomalous and (b) normal dispersion regimes, where the physical powers are normalized to the threshold ionization power P_{th}, i.e., $|\psi|_{\text{th}}^2 = 1$. When the normalized input power $\psi_0^2 \leq |\psi|_{\text{th}}^2$, the usual Kerr-related MI sidebands are seen, existing uniquely in the anomalous regime. However, when $\psi_0^2 > |\psi|_{\text{th}}^2$, plasma-induced MI causes the sidelobes to be unbounded and to have slowly decaying tails. A similar situation occurs in the normal regime, where the gain is slightly lower due to the absence of the Kerr contribution. For this case there are no instabilities below the threshold power since no plasma is generated.

Numerical simulations —To validate the analysis based on the simplified model given by Eqs. (1) and (2), and also to provide further insight into the dynamics of plasma-induced MI, UPPE simulations were performed [6]. The ionization rate was calculated using the Yudin-Ivanov model [8], which accurately describes both quasistatic tunneling and multiphoton ionization along with the

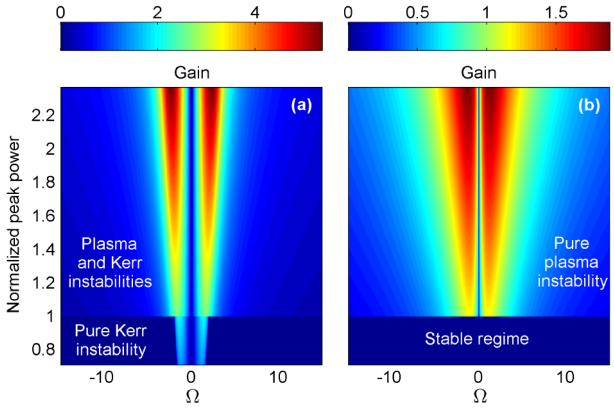

FIG. 2 (color online). MI spectral gain profile versus normalized input peak power in (a) anomalous and (b) normal dispersion regimes with equal magnitude of GVD. For the anomalous regime, a cw with $\lambda = 1064$ nm is launched into a kagome HC-PCF, core diameter 20 μm, filled with argon gas, the pressure of 1 bar, which gives $\beta_2 \simeq -2.8$ ps^2/km. In this fiber, $P_{\text{th}} \simeq 105$ MW at room temperature. All subsequent calculations in this Letter are based on this fiber. For the normal regime simulation, we assume hypothetically a gas-filled fiber with a β_2 of the same magnitude as in (a) but with a positive sign.

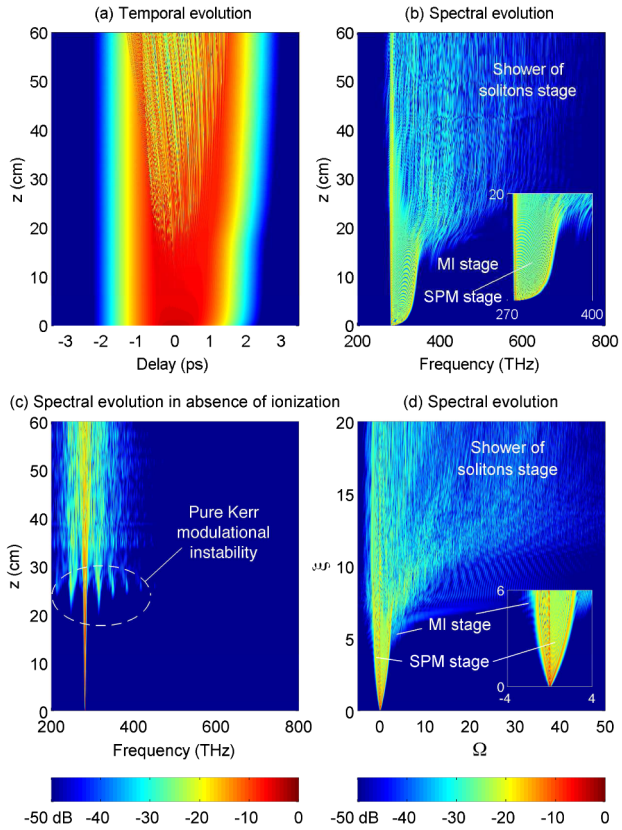

FIG. 3 (color online). Temporal (a) and spectral (b) intensity evolution of a long Gaussian pulse propagating in an Ar-filled HC-PCF, calculated using a UPPE. (c) The corresponding spectral intensity evolution in absence of ionization. (d) The spectral intensity evolution obtained by solving the coupled equations (1) and (2).

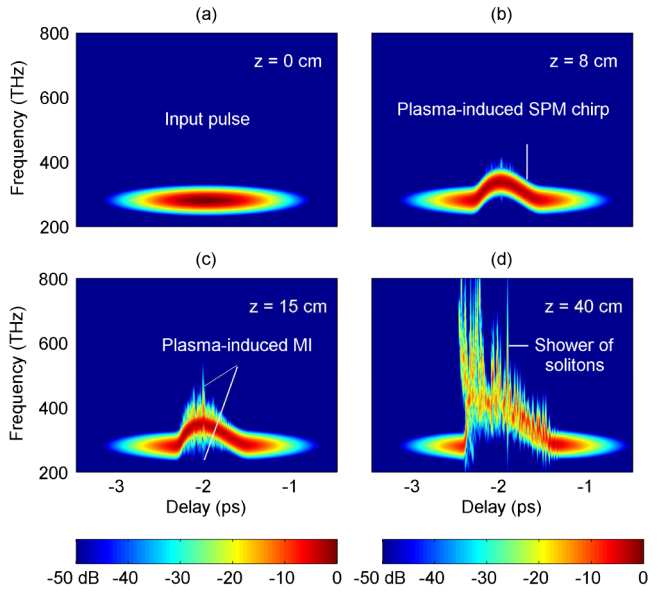

FIG. 4 (color online). Cross-frequency-resolved optical gating spectrograms for the propagation through an Ar-filled HC-PCF. The simulation parameters are the same as in Fig. 3. The reference pulse is a Gaussian with FWHM 50 fs. (a) Input pulse. (b) SPM frequency chirping. (c) Modulational instability. (d) Soliton disintegration into multiple blueshifting solitons.

transition between these regimes [8,23], and has been shown to agree well with experimental measurements [3,5].

Figures 3(a) and 3(b) show the temporal and spectral evolution of a Gaussian pulse at 1064 nm with duration 1.18 ps and peak power 200 MW through an Ar-filled HC-PCF. The pump pulse has a soliton number $N \simeq 102$, and its peak corresponds to a Keldysh parameter of $\gamma = 0.785$, and for most of the pulse $\gamma < 5$. This corresponds to the nonadiabatic tunneling regime [8]. The first stage of propagation shows asymmetric spectral broadening toward the blue due to ionization-induced SPM as described above—see Fig. 3(b) and inset. Immediately after the SPM stage, dispersion starts to play a role, and due to the combined Kerr and plasma-induced MIs, broad and slowly decaying sidelobes are generated and amplified quickly—see the oscillations in the time domain in Fig. 3(a). In the third and final stage in the propagation, strongly blueshifted solitons are emitted. For comparison, Fig. 3(c) shows propagation without ionization. In this case, weak sidelobes due to Kerr driven MI are visible, and there is no evidence of spectral asymmetry. In presence of ionization, the strong SPM process hides the instability bands in the frequency domain, as shown in Fig. 3(b). However, the instability is clearly visible in the time domain; see Fig. 3(a) after $z = 20$ cm. Figure 3(d) shows the spectral propagation obtained by solving the coupled equations (1) and (2). All of the qualitative features of the UPPE simulations are reproduced, validating this model and the subsequent analysis discussed in this Letter.

Further insight into the dynamics can be obtained from Fig. 4, which shows the evolution of the cross-frequency-resolved optical gating spectrograms of the pulse at different positions along the fiber. The pulse is initially asymmetrically chirped to high frequencies at its center [Fig. 4(b)] due to the higher plasma density created at the highest intensities. This is the plasma-induced SPM chirp described above. At the same time, two plasma-induced MI sidebands appear in the pulse spectrum [Fig. 4(c)], as discussed above. Plasma-induced MI facilitates the formation of many solitons. In less than half a meter of propagation, the initial pulse disintegrates into a "shower" of solitons, see Figs. 4(d), each undergoing a strong self-frequency blueshift induced by intrapulse photoionization, as described in detail in Refs. [9,10].

Conclusions—In this Letter, we have investigated analytically and numerically the propagation of intense and relatively long pulses in an Ar-filled kagome-style HC-PCF. Several surprising results have emerged, such as strongly asymmetric SPM, which could be studied analytically with the envelope equations (1) and (2), a universal type of plasma-induced MI, existing in both anomalous and normal dispersion for all frequencies and exhibiting long tails in the gain spectra, and the final disintegration of

the pulse into a multitude of blueshifting solitons, which form a plasma-induced continuum. All these regimes are realistically accessible in experiments. These theoretical results further highlight the stimulating new possibilities opened up by accessing the ionization regime in hollow-core photonic crystal fibers.

[1] P. St. J. Russell, Science **299**, 358 (2003).
[2] P. St. J. Russell, J. Lightwave Technol. **24**, 4729 (2006).
[3] J. C. Travers, W. Chang, J. Nold, N. Y. Joly, and P. St. J. Russell, J. Opt. Soc. Am. B **28**, A11 (2011).
[4] Y. Y. Wang, N. V. Wheeler, F. Couny, P. J. Roberts, and F. Benabid, Opt. Lett. **36**, 669 (2011).
[5] P. Hölzer, W. Chang, J. C. Travers, A. Nazarkin, J. Nold, N. Y. Joly, M. F. Saleh, F. Biancalana, and P. St. J. Russell, Phys. Rev. Lett. **107**, 203901 (2011).
[6] W. Chang, A. Nazarkin, J. C. Travers, J. Nold, P. Hölzer, N. Y. Joly, and P. St. J. Russell, Opt. Express **19**, 21018 (2011).
[7] P. Kinsler, Phys. Rev. A **81**, 013819 (2010).
[8] G. L. Yudin and M. Y. Ivanov, Phys. Rev. A **64**, 013409 (2001).
[9] M. F. Saleh, W. Chang, P. Hölzer, A. Nazarkin, J. C. Travers, N. Y. Joly, P. St. J. Russell, and F. Biancalana, Phys. Rev. Lett. **107**, 203902 (2011).
[10] M. F. Saleh and F. Biancalana, Phys. Rev. A **84**, 063838 (2011).
[11] E. M. Dianov, A. Ya. Karasik, P. V. Mamyshev, A. M. Prokhorov, V. N. Serkin, M. F. Stel'makh, and A. A. Fomichev, JETP Lett. **41**, 294 (1985).
[12] F. M. Mitschke and L. F. Mollenauer, Opt. Lett. **11**, 659 (1986).
[13] A. G. Bulushev, E. M. Dianov, O. G. Okhotnikov, and V. N. Serkin, JETP Lett. **54**, 619 (1991).
[14] M. N. Islam, G. Sucha, I. Bar-Joseph, M. Wegener, J. P. Gordon, and D. S. Chemla, Opt. Lett. **14**, 370 (1989).
[15] A. S. Gouveia-Neto, M. E. Faldon, and J. R. Taylor, Opt. Commun. **69**, 325 (1989).
[16] E. M. Dianov, A. B. Grudinin, D. V. Khaidarov, D. V. Korobkin, A. M. Prokhorov, and V. N. Serkin, Fiber and Integrated Optics **8**, 61 (1989).
[17] G. P. Agrawal, *Nonlinear Fiber Optics* (Academic Press, San Diego, 2007), 4th ed..
[18] S. C. Pinault and M. J. Potasek, J. Opt. Soc. Am. B **2**, 1318 (1985).
[19] A. L. Gaeta, Phys. Rev. Lett. **84**, 3582 (2000).
[20] A. Hasegawa and W. Brinkman, IEEE J. Quantum Electron. **16**, 694 (1980).
[21] K. Tai, A. Hasegawa, and A. Tomita, Phys. Rev. Lett. **56**, 135 (1986).
[22] K. Tai, A. Tomita, J. L. Jewell, and A. Hasegawa, Appl. Phys. Lett. **49**, 236 (1986).
[23] V. M. Gkortsas, S. Bhardwaj, C. J. Lai, K. H. Hong, E. L. Falcão-Filho, and F. X. Kärtner, Phys. Rev. A **84**, 013427 (2011).